EUROPEAN ORGANIZATION FOR NUCLEAR RESEARCH
European Laboratory for Particle Physics

Large Hadron Collider Project

LHC Project Report 950

Hardness and Tensile Strength of Multifilamentary Metal-matrix Composite Superconductors for the Large Hadron Collider (LHC)

C. Scheuerlein[1], T. Boutboul[1], D. Leroy[1], L. Oberli[1]
B. Rehmer[2]

Abstract

Conventional indentation hardness measurements to obtain load independent Vickers hardness values for the different phases in multifilamentary superconducting (SC) wires are described. The concept of composite hardness is validated for a binary metal-matrix metal-filament Nb-Ti/Cu composite wire. The tensile materials properties of the individual wire components are estimated from their indentation hardness. The potential and limitations of this approach are critically discussed, based on a comparison with tensile test results obtained for wires and extracted Nb-Ti filaments.

1 CERN, Accelerator Technology Department, Geneva, Switzerland
2 Bundesanstalt für Materialforschung und -prüfung (BAM), Berlin, Germany

To be published in Journal of Materials Science

CERN
CH - 1211 Geneva 23
Switzerland

Geneva, 14 July 2006

1 Introduction

The 220 000 km of superconducting (SC) wires [1] used for the fabrication of the LHC [2] accelerator magnet coils are composite materials in which the superconducting material is present in the form of small sized filaments. As an example, the wires used in the LHC inner dipole cables consist of 8900 Nb-Ti filaments with a diameter of 7 μm, embedded in the Cu matrix of the wire with a diameter of about 1 mm.

The determination of the materials constants for the individual phases in the superconducting composite wires is complicated by the small size of the different phases with typical cross sections of a few tens of μm^2 and because of a plastic and elastic anisotropy of the strongly textured materials. The goal of the present work is to assess whether it is possible to extract tensile properties of SC composite wires from indentation hardness measurements of their individual components.

For ductile metals the indentation hardness is basically a measure for the plastic materials properties and factors have been elaborated that allow to compare the Vickers hardness (HV) with the yield stress (YS). For fully work-hardened, isotropic metals for which elastic deformation can be neglected the uniaxial YS is about one third of the Vickers hardness (expressed in identical units) [3]. The correlation factor between hardness and YS decreases when elastic deformation becomes significant (for $E/YS<133$ or $E/HV<44.3$). For this case it has been found that the relation between HV and YS is given by [4,5]:

$$HV/YS=0.065+0.6\ln(E/YS) \qquad \text{Equation 1}$$

In the present article indentation hardness measurements in SC composite wires for the LHC are presented and their accuracy is assessed. The Nb-Ti/Cu indentation hardness data is compared with tensile test results, which has been obtained for single Nb-Ti filaments, Nb-Ti filament bundles and entire Nb-Ti/Cu composite wire samples. Based on the experimental results the possibility to predict the tensile composite wire properties from the indentation hardness and the possibility to extend this method to other SC designs is critically discussed.

2 Experimental

2.1 The samples

The samples analysed are Nb-Ti/Cu superconducting wires for the LHC. All samples have been manufactured in a single stack process, i.e. all Nb-Ti rods are stacked at once in a Cu extrusion billet. The nominal diameter, Cu and Nb-Ti volume fractions (the copper to superconductor ratio Cu/SC [6]) and the number and size of Nb-Ti filaments for the two sample types are summarised in Table I. A cross section of a 01 type wire sample is shown in Figure 1. The 02R wire is an outer LHC conductor with an intermediate diameter of 6.7 mm, which has not been drawn down to the nominal 02 wire diameter of 0.825 mm. The Nb-Ti and Cu hardness in this wire is measured before the precipitation heat treatment. The Nb-Ti cross sectional areas in the 02R wire are sufficiently large to measure the Nb-Ti hardness with relatively high indent load in order to obtain the load dependence of the hardness result.

The Nb-Ti filaments contain 47±1 wt.% Ti and only traces of other elements and the matrix is made of OFHC copper. During the SC composite wire fabrication the fully recrystallised Nb-47wt.%Ti alloy raw material is reduced by a series of extrusion and drawing processes down to the final SC filament size of 6-7 μm. In order to form a Nb-Ti microstructure that promotes a high critical current density, the composite wire undergoes the highest possible cold-work strain [7], which strongly increases the tensile strength of the filaments and the matrix.

During several hot fabrication processes the Nb-Ti filaments and the Cu matrix are strongly bonded with each other and in the following an ideal bond between both phases is assumed. The Nb-Ti filaments in the 01 wire have a twist pitch of 18 mm. In the 02R wire the filaments are not twisted.

Two different 01R wires were examined. The wire 01R010 is a pre-series wire, which final precipitation heat treatment lasts 2 times longer than that of the optimised LHC wire 01R152. At the end of the production the wires are submitted to a final 1 h-190 °C heat treatment, during which the Cu matrix is partly annealed.

2.2 Hardness measurements

Indentation hardness measurements have been done in transverse metallographic wire cross sections, which were prepared by wet grinding and mechanical polishing with various diamond suspensions. For the last polishing step a 0.1 μm colloidal silica suspension with pH=9 has been used. The thickness of the damaged surface layer remaining after the chemical polishing is estimated as about twice the final polishing particle size [8], i.e. 0.2 μm.

Conventional hardness measurements have been performed using a Leica VMHT MOT hardness tester using a Vickers diamond pyramid indenter. The test load was always applied during 15 s. Prior to the hardness measurements the instrument was calibrated using two polished stainless steel standard samples with nominal hardness HV0.5=712±17.4 and HV0.005=264±31.1. The respective hardness results measured with the Leica VMHT MOT are HV0.5=717±3.1 and HV0.005=254±10.6. Pile-up [3] in the cold worked copper is neglected in the calculation of HV from the indent diagonals.

2.3 Tensile tests of composite wires

Tensile tests on the entire composite wire 01R152 were performed according to [9]. The wire strain was measured with a commercially available clip on extensometer (INSTRON 2620-601) with a weight of 30 g. The gauge length was 50 mm and the tests were done with constant strain rate of 10^{-4} s^{-1}. As recommended in [9] the tensile test is stopped at 2 % elongation and the strain gauge dismounted after the stress had been released by 10 % in order to avoid damage of the strain gauge when the wire sample fractures. For the measurement of the ultimate tensile strength (R_m) the test was afterwards continued with constant stroke rate of 0.05 mm s^{-1} until strand rupture occurred.

E-moduli determined from the loading stress strain curve (E_0) are usually lower than E-moduli determined form the unloading stress strain curves (E_A). For Nb-Ti/Cu wire it has been shown that reliable E-modulus values can be obtained from the unloading curve, regardless the unloading stress level [10]. The 0.2% proof stress obtained from the unloading curve ($R_{p0.2B}$) is reported as a measure for the stress at which Cu yielding occurs.

2.4 Tensile tests of Nb-Ti filament bundles

Nb-Ti filament bundles were extracted from the Nb-Ti/Cu wires by dissolving the Cu matrix in HNO_3. The accuracy of the Nb-Ti filament bundle cross sectional areas presented in Table 1 is better than 1 % [6].

R_m of single Nb-Ti filaments has been determined with a force resolution of 1 mN. Prior to the tensile test the single filament cross sections were measured with an optical system using a Laser. The measurement of the filament cross sectional area is the main uncertainty of the single filament tensile test results.

3 Results

3.1 Vickers hardness measurements in transverse wire cross sections

3.1.1 HV load dependence

An important advantage of the Vickers hardness scale as compared to Brinell hardness is that Vickers hardness results are considered to be load-independent (principle of geometric similarity [3]). However, this is the case only when the applied indent load exceeds typically 100 gf (1 gramforce = 9.81 mN).

For a variety of different reasons HV measurements in the low load range depend on the indent load. Most instrumental artefacts (e.g. vibrations, friction within tester, indent size measurement errors) occur with conventional indentation instruments and can be largely avoided when using instrumented indentation testers with a sophisticated insulation against mechanical and acoustic vibrations. Other artefacts are related to indenter imperfections. A further artefact that can cause a dramatic HV increase at low loads is sample surface workhardening by the mechanical polishing, which might be avoided by electropolishing the sample surface. Electropolishing is, however, not obvious to achieve for multi phase samples. Finally there is a true hardness increase with decreasing indentation depth. This HV increase becomes important for indent depths smaller than 300 nm, which per definition is the border between micro and nanoindentation.

In Figure 2 the HV load dependence is shown for the cold worked Nb-Ti alloy and Cu matrix in the 02R wire cross section. With decreasing load HV values increase until they drop again at very low loads (1 gf). Such a HV load behaviour is typically obtained with conventional indentation testers [11] without sophisticated isolation against environmental vibrations.

3.1.2 The concept of Nb-Ti/Cu composite hardness

Hardness measurements in metallographic wire cross sections were also performed with higher loads such that the indents were penetrating a large number of Nb-Ti filaments and the Cu matrix. The results of these HV measurements are in the following referred to as the Nb-Ti/Cu composite hardness. In analogy to the concept of composite hardness used for the calculation of the hardness of thin films on substrates with differing hardness [8], below the Nb-Ti filament hardness ($HV_{Nb\text{-}Ti}$) is calculated from the Cu matrix hardness (HV_{Cu}), the Nb-Ti/Cu composite hardness ($HV_{composite}$) and the corresponding volume fractions V_{Cu}/V_{total} *and* $V_{Nb\text{-}Ti}/V_{total}$ in the composite according to:

$$HV_{composite}=HV_{Cu}*V_{Cu}/V_{total}+HV_{Nb\text{-}Ti}*V_{Nb\text{-}Ti}/V_{total} \qquad \textit{Equation 2}$$

In Table II the average HV values obtained for the Cu matrix, the Nb-Ti filaments and the Nb-Ti/Cu composite are shown. The Cu to Nb-Ti volume ratio in the composite wire part is $V_{Cu}/V_{Nb\text{-}Ti}=0.5$ (not taking into account the pure Cu part of the wire surrounding the Nb-Ti/Cu part).

The HV0.005 values obtained by direct indentation in the Nb-Ti filaments of samples 01R010 and 01R152 exceed the corresponding Nb-Ti hardness values calculated from the composite hardness by between 3 and 4 %, which is explained by the load dependence of the HV0.005 results (see Figure 2). The 10 gf indent diagonals in the Nb-Ti filaments have a length of almost 6 µm and are therefore in contact with the Nb-Ti/Cu interface. Due to the increasing influence of the Cu matrix on the Nb-Ti hardness result the HV0.01 result for the Nb-Ti filaments is about 2 % lower than the Nb-Ti hardness calculated from the composite hardness.

The Nb-Ti/Cu composite hardness was probed with loads up to 500 gf and load independent results were obtained with a minimum load of 200 gf (see Figure 3).

3.2 Tensile tests

3.2.1 Tensile tests of Nb-Ti/Cu composite wires

A stress-strain curve obtained for the Nb-Ti/Cu wire 01R152 is shown in Figure 4. The 0.2 % proof stress due to Cu yielding ($R_{p0.2A}$ and $R_{p0.2B}$), the second order 0.2% proof stress ($R_{p0.2C}$), which indicates yielding of the Nb-Ti filaments, and the elastic modulus (E_0 and E_A) are defined as described in [9]. The reinforcing Nb-Ti filaments have a lower E-modulus and a higher yield strength than the Cu matrix. Therefore, one observes two linear parts in the stress-strain curve, the first until Cu starts to yield plastically and the second until plastic Nb-Ti yielding occurs [12].

The tensile test results are summarised in Table III. The values presented are average values obtained for 8 wire samples. The E-modulus measured with increasing load is usually somewhat lower than the E-modulus measured with decreasing load (in the present case 99.2±6.0 GPa and 105±2 GPa, respectively). $R_{p0.2B}$ is with 282±8 MPa about 4 % lower than $R_{p0.2A}$.

3.2.2 Tensile tests of single Nb-Ti filaments and Nb-Ti filament bundles

Two stress-strain curves obtained for filament bundles extracted from samples 01R152 and 01R010 are shown in Figure 5. The R_m and E_0 values that have been measured for the Nb-Ti filament bundles and R_m obtained for single Nb-Ti filaments are shown in Table IV.

The E-modulus and tensile strength of the Nb-Ti filaments in the different wires differ markedly. The E-modulus of the filaments in the 01R152 wire agrees well with the literature value of $E_{Nb\text{-}47wt.\%Ti}$=87 GPa [5]. The Nb-Ti filament E-modulus for the 01R010 wire is 11 % higher than it is for the filaments extracted from wire 01R152. The filaments extracted from both samples do hardly exhibit any plasticity up to rupture.

The discontinuous stress-strain behaviour at high stress is partly caused by slight differences in the cross section of individual filaments within a filament bundle. Due to these differences some of the extracted filaments will fracture at lower loads than others, thus reducing the total Nb-Ti cross section at maximum load. Since the tensile strength is

calculated with the cross sectional area of all filaments, tensile tests of ductile filaments give a minimum value for the tensile strength, which can be more or less exceeded when the tensile strength is based on the true filament cross section, as it is done when doing single filament tensile tests.

A comparison between R_m results obtained for the two different filament bundle samples shows that the tensile strength of the filaments in sample 01R152 exceeds the strength of the filaments in sample 01R010. This is confirmed by the R_m results found for the entire composite wires, which show that the 01R010 wire has a lower strength than the 01R152 wire.

The average R_m value that has been obtained for 6 individual Nb-Ti filaments that were extracted from the wire 01R152 is 1302±297 MPa. The large scatter in these results is mainly due to uncertainties in the filament cross section measurement. The rounded value of R_m=1300 MPa will be used in the following. In [13] an average R_m value of 1240 MPa is reported for Nb-Ti filaments extracted from Nb-Ti/Cu composite wires.

4 Discussion

4.1 Indentation hardness measurements in SC wire cross sections

4.1.1 Dependence of HV results on the indent load

For the determination of the tensile strength from HV values, the hardness result must be load independent. The influence of indent load depends on the material and its degree of cold-work. As outline above, the load dependence of HV results is caused by instrumental uncertainties (increasing influence of vibrations on HV with decreasing indent load), sample preparation artefacts and a true hardness increase with decreasing indentation depth [14]. For metallographically prepared copper it has been shown that the strong hardness increase at very low loads is mainly caused by the work-hardening of a surface layer during mechanical polishing [15].

As shown in Figure 2 a minimum indent load of 15 gf is required in order to obtain load-independent hardness results for the cold worked Nb-47wt.%Ti alloy. On the other hand

for direct indentation in the Nb-Ti filaments of the LHC wires the indent load must not exceed 5 gf in order to avoid a strong influence of the surrounding Cu on the hardness result. Hence, it is impossible to obtain accurate, i.e. load independent results for the filaments in LHC wires by direct indentation measurements. Therefore, the concept of composite hardness is adopted for the measurement of the Nb-Ti filament hardness.

4.1.2 Calculation of filament hardness from composite hardness

For the LHC SC composite wires the Nb-Ti hardness can be determined accurately from the composite hardness results, the hardness of the interfilamentary copper and the volume fractions for Cu and Nb-Ti filaments. The interfilamentary Cu hardness can not be measured directly and it is assumed that it equals the hardness of the Cu outside the filament area. Errors in the interfilamentary Cu hardness have a comparatively small influence on the calculated Nb-Ti hardness (e.g. an error of 10 % in the Cu hardness causes and error in the Nb-Ti hardness of 1.5 %). The composite hardness can be measured with a sufficiently high load so that problems and artefacts related to low indent loads are avoided.

The Nb-Ti/Cu interfaces represent obstacles for the dislocation movement. Therefore, when the dimensions of the filaments and the interfilamentary spacing are reduced such that they approach the dimensions of other dislocation obstacles like the grain boundary spacing, the size effect gets an increasingly important influence on the mechanical properties. A strong size effect has for instance been observed in Nb/Cu binary composite wires with a filament spacing of 45 nm [16], causing a strongly increased interfilamentary Cu tensile strength.

If there would be a strong size effect on the strength of the LHC wires, the Nb-Ti hardness measured by direct indentation of an individual filament should be lower than the Nb-Ti hardness calculated from the composite hardness. Since this is not the case (see Table II) it is concluded that there is no significant size effect on the composite hardness measured in the LHC wire cross sections, with Nb-Ti filament diameters between 6 and 7 μm and a spacing of about 1 μm. In [17] no size induced effect was observed for

filaments exceeding 10 μm, while at lower dimensions an increase in hardness is observed, which is attributed to Hall-Petch strengthening.

4.2 Indentation hardness and tensile strength of the individual wire components

As outlined above, for an ideal fully work hardened polycrystalline metal without any preferred crystalline orientation the YS can be determined from the correlation YS=HV/3, or when elastic deformation is significant the YS is given by Equation 1. However, in the Nb-Ti/Cu wires above conditions are not fulfilled for both components.

4.2.1 Indentation hardness and tensile strength of the Cu matrix

The Cu matrix of the LHC wires is partly annealed during the final 1 h-190 °C heat treatment and, therefore, during the indentation process Cu will undergo additional work hardening. As a result, the Cu matrix YS can not be determined from indentation hardness measurements. However, the measured Cu hardness is an indication for the degree of cold work in the Cu matrix and the corresponding YS values may be found in literature.

In Table V the YS and R_m found for Cu with different degrees of cold-work is shown. For isotropic Cu with HV=87 (about the hardness measured for the Cu matrix in the LHC SC wires) a YS of 270 MPa and R_m of 314 MPa is reported [24]. In the following these values are used for rule of mixture (ROM) calculations.

4.2.2 Indentation hardness and tensile strength of the Nb-Ti filaments

It has been shown that the Nb-Ti filaments in Nb-Ti/Cu wires are strongly textured [13]. This anisotropy can cause a significant deviation from the HV/YS ratio as it is valid for isotropic materials.

In Table VI the mechanical properties of the Nb-Ti filaments of the two different 01R samples are summarised and the measured tensile strength is compared with the tensile strength calculated from HV and the E-modulus according to Equation 1.

For the fully annealed Nb-47wt.%Ti alloy raw material the YS and R_m are about 380 and 400 MPa, respectively. It can be expected that the difference between YS and R_m decreases with increasing cold work. From the stress-strain curves obtained for extracted filament bundles (see Figure 5) it can also be seen that the extracted filaments deform almost entirely elastically until rupture occurs and, for the heavily cold worked free standing Nb-Ti filaments differences between YS and R_m are in the following neglected.

Hence, it can be concluded that the tensile strength of the strongly textured Nb-Ti filaments calculated according to Equation 1 is significantly lower than R_m determined experimentally for the free standing single filaments (10 % with respect to the filament bundle R_m and about 20 % as compared to the single filament R_m in the case of the 01R152 sample). In addition, R_m of the Nb-Ti filament bundle extracted from wire 01R152 (1160±31 MPa) is more than 20 % higher than R_m of the 01R010 filament bundle (902±57 MPa), while the difference in the tensile strength calculated according to Equation 1 does not show a strong difference in both cases.

It has been shown that in the approximate hardness range HV=[150,270] there is a nearly linear dependence between the Vickers hardness of the Nb-46.5wt.%Ti alloy and the true strain to which it is subjected [18]. From the data presented in this article and elsewhere it appears that there is a saturation of the Nb-Ti indentation hardness at approximately HV=290, while the uniaxial tensile strength continues to increase with increasing cold work [19].

4.2.3 Different mechanical behaviour of Nb-Ti filaments due to different heat treatments

There are at least two possible reasons why the mechanical properties of the Nb-Ti filaments change with increasing heating time, notably a different degree of texture and an increasing content of α-Ti precipitates.

Similar relative variations of Nb-Ti E-moduli as they are reported here have been found by tensile tests of single Nb-Ti filaments that were subjected to different heat treatments [19]. The differences have been attributed to a different content of α-Ti precipitates in the filaments (after identical degree of cold work the α-Ti content increases with heat

treatment temperature and time). It was concluded that the higher the α-Ti content the higher is the Nb-Ti alloy E-modulus. Another explanation for the different elastic behaviour may be a differently strong elastic anisotropy due to a different degree of texture.

Differences in R_m after the different heat treatments could also be attributed to a different α-Ti precipitate concentration and the size and spacing of the individual α-Ti precipitates within the Nb-Ti alloy. However, if such differences influence the tensile strength they should also influence the indentation hardness. Therefore, it is assumed that the different tensile strength found for both wire samples is mainly caused by a different degree of texture in the filaments, which influences the tensile strength but not the indentation hardness.

The difference in the E-modulus and tensile strength of the Nb-Ti filaments in both 01R wires that have been investigated is therefore explained by different wire heat treatments, notably the 2 times longer final α-Ti precipitation heat treatment time to which the pre-series 01R010 wire was submitted.

4.3 Calculation of tensile properties according to the rule of mixtures (ROM)

Below the tensile properties E-modulus and R_m are calculated according to the ROM from the tensile properties that have been determined for the entire composite wires and the extracted Nb-Ti filaments, assuming isostrain conditions.

4.3.1 Calculation of the Cu E-modulus according to the ROM

It has been shown for a variety of multifilamentary SC wires that E-modulus values elaborated from tensile tests follow the ROM within the accuracy of the experimental results [12]. Hence, from the E-modulus values E_{wire} and $E_{Nb\text{-}Ti}$ the Cu matrix E-modulus can be calculated with the corresponding volume fractions $V_{Nb\text{-}Ti}/V_{total}$=0.374 and V_{Cu}/V_{total} =0.626 according to:

$$E_{Cu} * V_{Cu}/V_{total} = E_{wire} - E_{Nb\text{-}Ti} * V_{Nb\text{-}Ti}/V_{total} \qquad \textit{Equation 3}$$

The calculated values for the Cu E-modulus of 116 GPa in the two 01R wires (see Table VII) are similar to the literature value of 119 GPa, which is reported in [5] for 60 % cold-drawn OFHC copper in Nb-Ti/Cu composites. An E-modulus of 118 GPa has been determined for the Cu matrix in an internal tin Nb_3Sn multifilamentary SC wire [20].

The E-modulus of 116 GPa for the Cu in the Nb-Ti/Cu wire determined from tensile test results confirms also previous findings on the elastic anisotropy of cold worked Cu by ultrasonic methods [21, 22], which report for strongly deformed Cu an E-modulus reduction of up to 11 % as compared to fully annealed texture free Cu, which has an E-modulus of 128 GPa. This elastic stiffness reduction has been attributed to texture that is formed during the Cu deformation [21].

4.3.2 Estimation of the wire R_m according to the ROM

For the application of the ROM for the calculation of the tensile wire strength several assumptions must be made [12]. Among others it is assumed that there are no transverse stresses in the loaded composite and that there are no residual stresses in the different phases of the unloaded composite. In particular these two assumptions are not fulfilled and it is therefore of interest if the ROM can also be applied for the estimation of the tensile composite wire strength.

With R_{mCu}=314 MPa, $R_{mNb\text{-}Ti}$=1300 MPa, V_{Cu}/V_{total} =0.626 and $V_{Nb\text{-}Ti}/V_{total}$=0.374 the 01R152 wire ultimate tensile strength R_{mWire} is estimated according to Equation 4 as 683 MPa, which is 9 % lower that the experimentally obtained value of 747 MPa.

$$R_{m\text{-}wire} = R_{mCu} * V_{Cu}/V_{total} + R_{mNb\text{-}Ti} * V_{Nb\text{-}Ti}/V_{total} \qquad \textit{Equation 4}$$

A difference of some 10 % between ROM calculation and experimental result can be explained by the fact that the R_m of the filaments within the Cu matrix exceeds R_m of the individual free standing Nb-Ti filaments, since the Cu matrix stabilizes the filaments, thus allowing multiple necking of the embedded Nb-Ti filaments [**Error! Bookmark not defined.**].

R_m for the free standing Nb-Ti filaments extracted from sample 01R152 is about 1300 MPa and the increase of tensile strength (ΔR_m) due to the filament stabilisation within the matrix may be estimated from $R_{m\text{-}Cu}$ =314 MPa, $R_{m\text{-}wire}$=747 MPa and the volume

fractions V_{Cu}/V_{total} =0.626 and $V_{Nb\text{-}Ti}/V_{total}$ =0.374. Taking into account some additional Cu work hardening it is estimated that $\Delta R_m \approx 100$ MPa.

5 Conclusion

The methodology of indention hardness measurements for the estimation of plastic properties of the different wire phases has been described and the limitations of this approach have been discussed:

- Accurate load-independent HV values for the Nb-Ti filaments in multifilamentary SC wires can be elaborated from the Nb-Ti/Cu composite hardness.
- For the determination of the HV/YS ratio the materials E-moduli must be known. In the present case of binary composite Nb-Ti/Cu wires the Nb-Ti E-modulus can be obtained from tensile tests of extracted Nb-Ti filament bundles and the Cu E-modulus can be calculated according to the ROM.
- The materials anisotropy that is developed during wire processing can cause significant errors in the determination of the YS when using HV/YS ratios that are valid for isotropic materials and it is therefore preferable to probe the individual phases by tensile tests.

The measurement of indentation hardness remains as a comparatively simple method for assessing the plastic materials properties of all composite wire phases that can not be tested individually by tensile tests. Currently this method is applied for studies of the mechanical properties of non-reacted Nb_3Sn SC wires that are being developed in the context with the Next European Dipole (NED) project [23].

Acknowledgements

We are grateful to L. Thilly from LMP Poitiers for helpful discussions and to M. Bistritz, G. Kalinka, M. Finn and S. Glaubitz from the BAM for tensile testing of single Nb-Ti filaments and Nb-Ti composite wire samples.

Tables

Table I: Geometry of inner (01R) and outer (02R) LHC dipole SC composite wire samples [2]. Two 01R samples (01R152 and 01R010) have been tested. Sample 02R is an outer conductor drawn down to 6.7 mm diameter, measured before the final wire heat treatment.

Sample	Ø (mm)	No. of Nb-Ti filaments	Nominal filament Ø (μm)	Cu/SC	Cu area (mm^2)	Nb-Ti area (mm^2)
01R	1.065±0.003	≈8900	≈7	1.67	0.557 (62.6 vol.%)	0.333 (37.4 vol.%)
02R	6.7	≈6500	≈49	1.95	23.3 (66.1 vol.%)	11.9 (33.9 vol.%)

Table II: HV measured for the Cu matrix (HV_{Cu}*), the Nb-Ti filaments (*$HV_{Nb\text{-}Ti}$*) and the Nb-Ti/Cu composite (*$HV_{composite}$*). The calculated Nb-Ti hardness is obtained from* $HV_{composite}$, HV_{Cu} *and the respective volume fractions (*$V_{Cu}/V_{Nb\text{-}Ti}=0.5$*). Single phase and composite HV results are average values obtained for 5 and 3 measurements, respectively.*

Sample	HV_{Cu}	$HV_{composite}$	$HV_{Nb\text{-}Ti}$	*Nb-Ti calculated*
01R152	HV0.05=79.7±2.0	HV0.5=211±5.0	HV0.005=288±18 HV0.01=270±6	HV=277
01R010	HV0.05=94.4±2.6	HV0.5=221±4.4	HV0.005=294±27	HV=287

Table III: Tensile properties of two 01R LHC Nb-Ti/Cu composite wires. The E-modulus and 0.2 % proof stress are obtained from the unloading stress-strain curve. Results are average values obtained for 8 valid measurements.

Sample	*E_A (GPa)*	*$R_{p0.2B}$ (MPa)*	*$R_{p0.2C}$ (MPa)*	*R_m (MPa)*	*Elongation at fracture (%)*
01R152	104.6±1.9	282±8	687±6	747±8	3
01R010	108.6±0.5	n.m.	n.m.	720±1	2

Table IV: E_0 and R_m measured for Nb-Ti filament bundles and R_m of Nb-Ti single filaments extracted from 01R152. Results are average values obtained for at least 6 valid measurements.

Sample	*Nb-Ti filament bundle E_0 (GPa)*	*Nb-Ti filament bundle R_m (MPa)*	*Nb-Ti single filament R_m (MPa)*
01R152	85±4	1160±31	1302±297
01R010	96±9	902±57	n.m.

Table V: HV, YS and R_m found in literature for Cu with different degrees of cold work.

Reference	*HV*	*YS (MPa)*	*R_m (MPa)*
[3]	81	261	
[24]	49	54	224
	87	270	314

Table VI: Comparison between tensile Nb-Ti properties determined experimentally from filament bundles (R_m-bundles) and single filaments (R_m-single) and the Nb-Ti tensile strength calculated (R_m-calc.) from HV and E according to Equation 1. It is assumed that differences between YS and R_m for the Nb-Ti filaments can be neglected.

Sample	*E filament (GPa)*	*HV (MPa)*	*E/HV*	*HV/YS*	*R_m-calc. (MPa)*	*R_m-bundle (MPa)*	*R_m-single (MPa)*
01R152	85±4	2750	30.9	2.61	1050	1160±31	1302±297
01R010	96±9	2820	34.1	2.79	1010	902±57	n.m.

Table VII: Elastic properties of two Nb-Ti/Cu wires. The composite wire and Nb-Ti filament E-moduli have been determined experimentally and the Cu E-modulus is calculated according to the ROM assuming isostrain conditions.

Sample	*Composite wire E-modulus (GPa)*	*Nb-Ti filament E-modulus (GPa)*	*Cu E-modulus calculated according to ROM (GPa)*
01R152	104.6±1.9	85±4	116.3
01R010	108.6±0.5	96±9	116.1

Figures

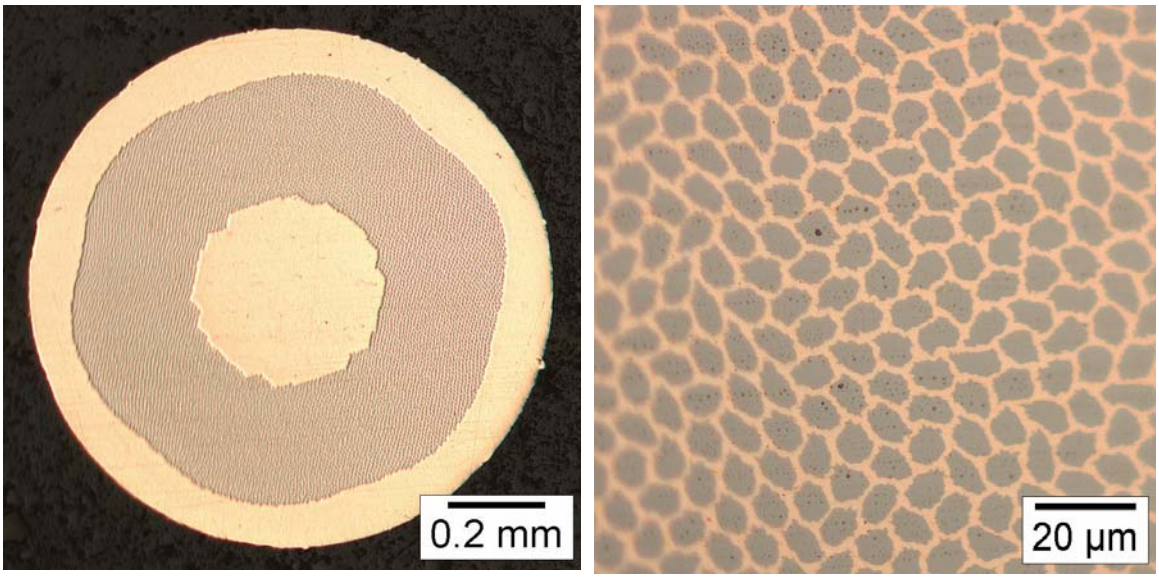

Figure 1: Transverse cross section of composite Nb-Ti/Cu wire 01R152 from which filaments were extracted for single filament tensile tests.

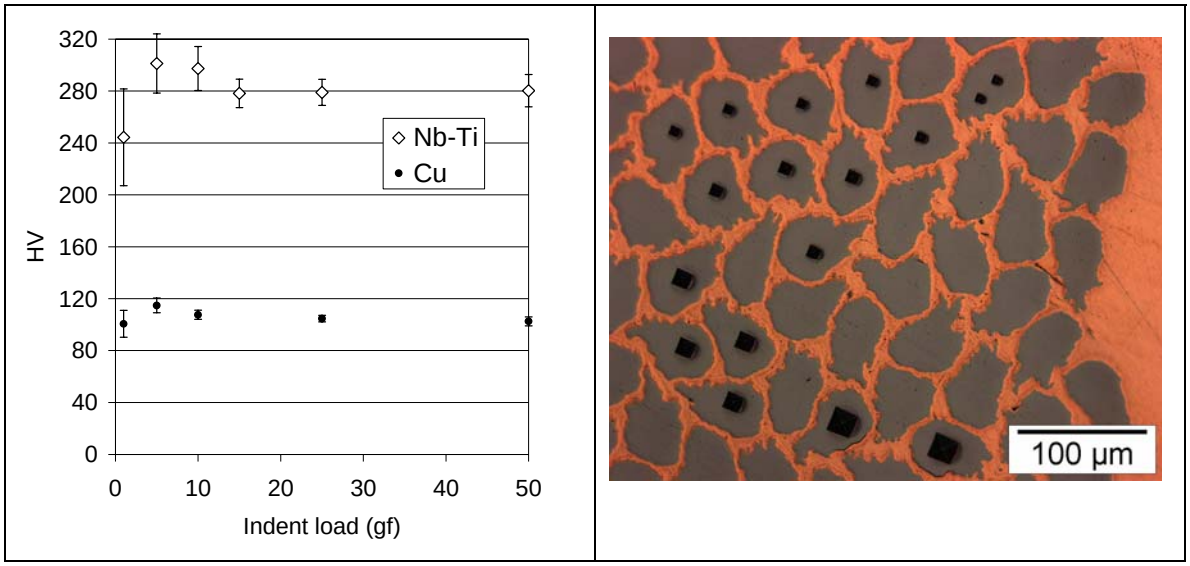

Figure 2: HV load dependence for cold-worked OFHC copper and Nb-47wt.%Ti alloy in the 02R Nb-Ti/Cu transverse wire cross section (wire diameter 6.7 mm). The HV values are the average result obtained from five measurements. The error bars represent one standard deviation. The decrease of HV values at very low load is caused by vibrations. In the right image the indents (10-100 gf) in the Nb-Ti filament cross sections of sample 02R are shown.

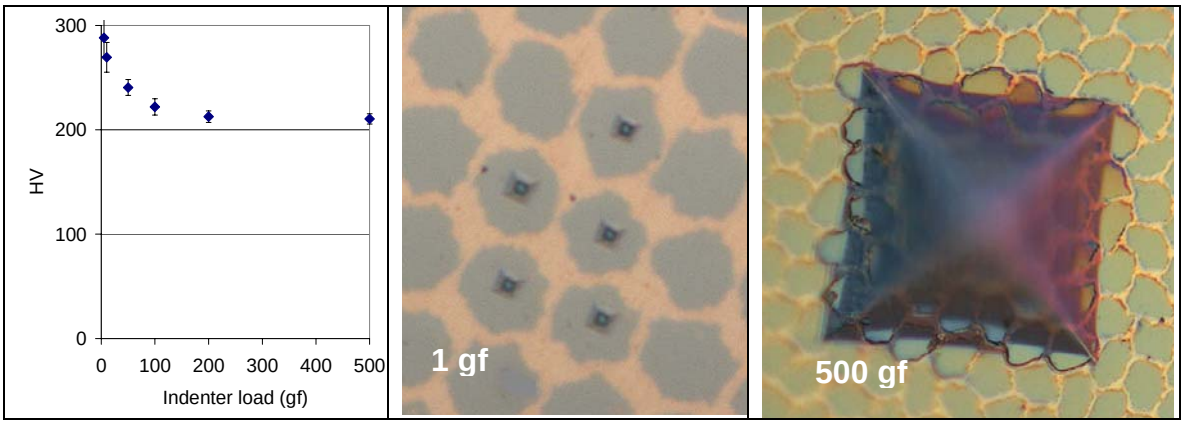

Figure 3: Variation of the HV result as a function of the indent load in the Nb-Ti/Cu composite region of sample 01R152. At 1 gf the HV result is only influenced by the Nb-Ti hardness and with increasing indent load the influence of the Cu matrix on the HV result increases. The Nb-Ti/Cu composite hardness is obtained with a minimum load of 200 gf. The corresponding Vickers indents within the individual Nb-Ti filaments (1 gf) and in the Nb-Ti/Cu composite (500 gf) in sample 01R152 are also shown.

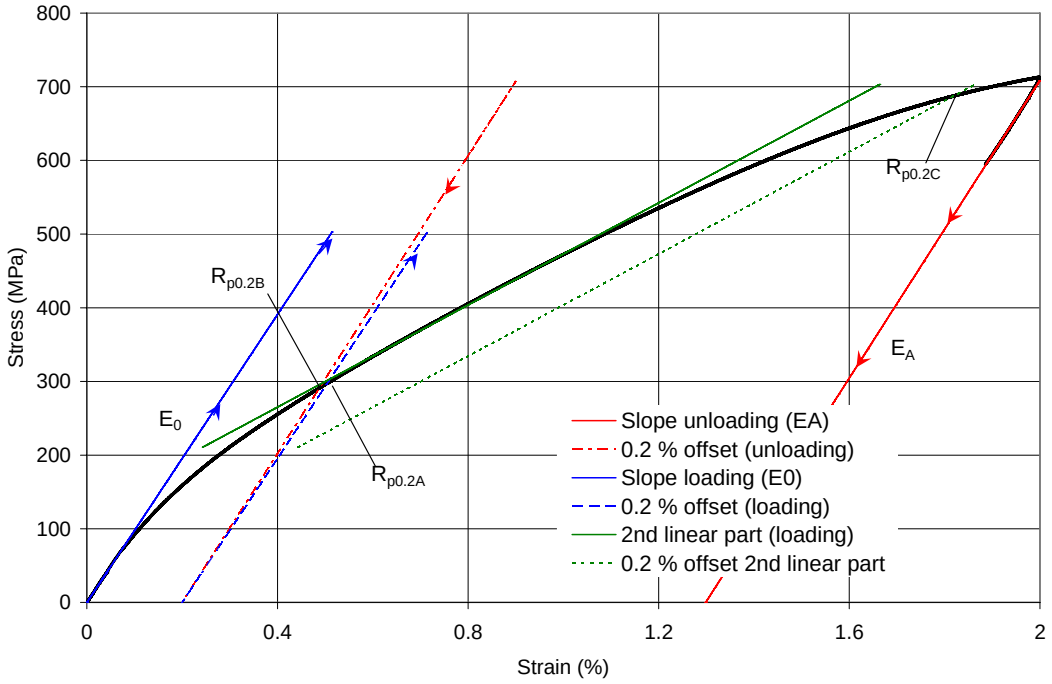

Figure 4: Stress strain curve obtained for the Nb-Ti/Cu wire 01R152 and definition of $R_{p0.2A}$, $R_{p0.2B}$, $R_{p0.2C}$, E_0 and E_A.

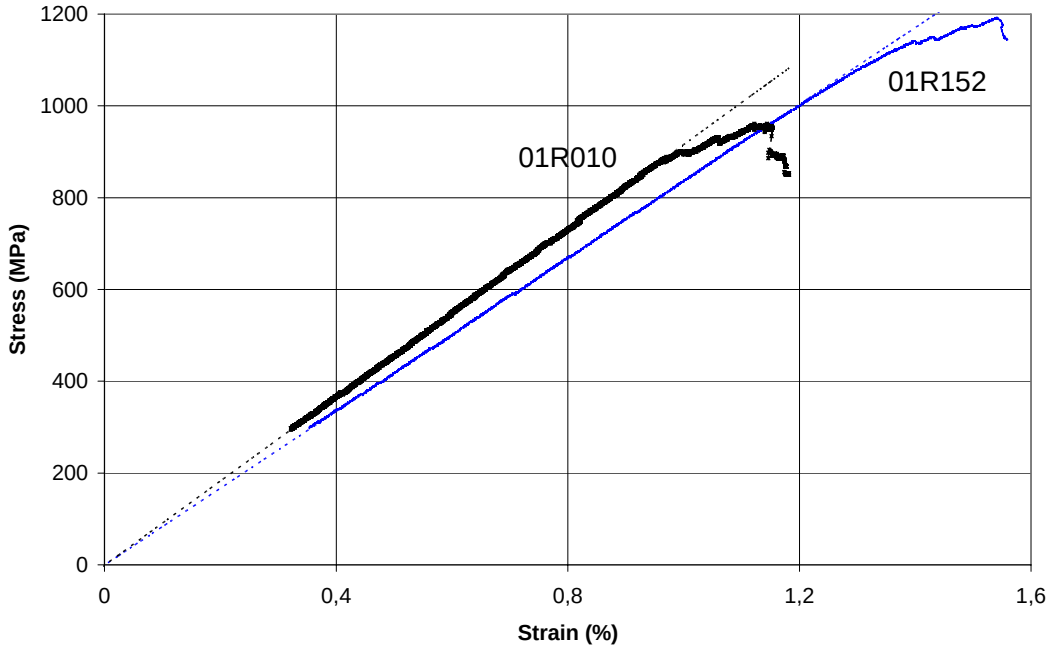

Figure 5: Stress-strain curve for Nb-Ti filament bundles extracted from the composite wires 01R152 and 01R010. The filaments of sample 01R010 have a higher E-modulus and a lower tensile strength than the filaments extracted from sample 01R152. It can be seen that the Nb-Ti filaments do hardly exhibit any plasticity up to rupture. The discontinuous stress-strain behaviour at high loads is probably caused by small variations in the cross sectional area of the individual filaments within the bundles.

References

1 J.D. Adam, T. Boutboul, G. Cavallari, Z. Charifoulline, C.H. Denarie, S. Le Naour, D.F. Leroy, L.R. Oberli, D. Richter, A.P. Verweij, R. Wolf, IEEE Trans. Appl. Supercond. 12(1), (2002), 1056

2 LHC Design Report Vol.1, "*The LHC Main Ring*", edited by O. Brüning, P. Collier, P. Lebrun, S. Myers, R. Ostojic, J. Poole, P. Proudlock, CERN-2004-003, (2004)

3 D. Tabor, "*The hardness of solids*", Review of Physics in Technology 1, (1970), 145-179

4 D.M. Marsh, "Plastic flow in glass", Proc. Roy. Soc. A, Vol. 279, (1963), 420-435

5 E.W. Collings, "*Applied Superconductivity, Metallurgy, and Physics of Titanium Alloys*", Vol.1, Plenum Press, New York, (1986)

6 T. Pyon, W.H. Warnes, M. Siddall, "Evaluation of Cu:SC ratio measurements by chemical etching, electrical resistivity, and image analysis", IEEE Trans. Appl. Supercond. 3(1), (1993), 1018

7 P. Lee, D. Larbalestier, "Niobium-titanium superconducting wires: Nanostructures by extrusion and wiredrawing", Wire Journal International 36(2), (2003), 61-66

8 H. Schumann, H. Oettel, "*Metallografie*", 14th edition, Willey-VCH, Weinheim, (2004)

9 International standard, DIN EN 61788-6(2001-07), "*Room temperature tensile test of Cu/Nb-Ti composite superconductors", (2001)*

10 K. Osamura, A. Nyilas, M. Shimada, H. Moriai, M. Hojo, T. Fuse, M. Sugano, "Definition of mechanical properties assessed by room temperature tensile test for the Cu/Nb-Ti composite wires", Proceeding of the 11th International Symposium on Superconductivity, Fukuoka, (1999), 1515

11 "Microhardness Testing", in ASM handbook Vol. 8, "Mechanical Testing", (1985)

12 C.C. Koch, D.S. Easton, "A review of mechanical behaviour and stress effects in hard superconductors", Cryogenics, (1977), 391-413

13 N. Iwasaki, M. Hojo, S. Ochiai, M. Ono, S. Sakai, K. Watanabe, "Structure observed by neutron diffraction, mechanical behaviour and critical current of multifilamentary Nb-Ti/Cu superconducting composite wire", J. Japan Inst. Metals 61(9), (1997), 792-800

14 W.D. Nix, H. Gao, "Indentation Size Effects in Crystalline Materials: A Law for Strain Gradient Plasticity", J. Mech. Phys. Solids, Vol.46(3), (1998), 411

15 Y. Liu, A.H.W. Ngan,"Depth dependence of hardness in copper single crystals measured by nanoindentation", Scripta mater. 44 (2001), 237-241

16 L. Thilly, P.O. Renault, V. Vidal, F. Lecouturier, S. Van Petegem, U. Stuhr, H. Van Swygenhoven, "Plasticity of multiscale nanofilamentary Cu/Nb composite wire during

in-situ neutron diffraction: Codeformation and size effect", Applied Physics Letters 88, (2006)

17 L. Thilly, F. Lecouturier, J. von Stebut, "Size-induced enhanced mechanical properties of nanocomposite copper/niobium wires: nanoindentation study", Acta Materialia 50, (2002), 5049-5065

18 J.A. Parrell, P.J. Lee, D.C. Larbalestier, "Cold Work Loss During Heat Treatment and Extrusion of Nb-46.5wt.%Ti Composites as Measured by Microhardness", IEEE Trans. Appl. Supercon., 3(1), (1993), 734-737

19 Z. Guo, W.H. Warnes, "Mechanical Behaviour of Fine Filament Nb-Ti as a Function of Processing", IEEE Trans. Appl. Supercond. 3(1), (1993), 1022

20 C. Scheuerlein, B. Rehmer, "Tensile properties of a non-reacted internal tin Nb_3Sn composite wire calculated from the Vickers hardness of its individual components according to the rule of mixtures", CERN, AT-MAS technical note 2005-08, EDMS 673338, (2005)

21 S.R. Agnew, J.R. Weertman, "The influence of texture on the elastic properties of ultrafine-grain copper", Materials Science and Engineering A242, (1998), 174-180

22 H.M. Ledbetter, S.A. Kim, "Low Temperature Elastic Constants of Deformed Polycrystalline Copper", Materials Science and Engineering A, 101, (1988), 87-92

23 A. Devred et.al., "Status of the Next European Dipole (NED) Activity of the Collaborated Accelerator Research in Europe (CARE) Project", IEEE Trans. Appl. Supercon. 15(2), (2005), 1106-12

24 Goodfellow product information
(http://www.goodfellow.com/csp/active/STATIC/G/Kupfer.HTML)